Journal of Alloys and Compounds 489 (2010) 228–232

Contents lists available at ScienceDirect

Journal of Alloys and Compounds

journal homepage: www.elsevier.com/locate/jallcom

Effects of Ag doping on thermoelectric properties of Zn_4Sb_3 at low temperatures

L. Pan, X.Y. Qin*, M. Liu, F. Liu

Key Laboratory of Materials Physics, Institute of Solid State Physics, Chinese Academy of Science, 230031 Hefei, People's Republic of China

ARTICLE INFO

Article history:
Received 5 June 2009
Received in revised form
10 September 2009
Accepted 10 September 2009
Available online 19 September 2009

Keywords:
Metals and alloys
Powder metallurgy
Electrical transport
X-ray diffraction

ABSTRACT

The thermoelectric properties of Ag-doped compounds $(Zn_{1-x}Ag_x)_4Sb_3$ ($x = 0$, 0.0025, 0.005, 0.01) have been studied at the temperatures from 15 to 300 K. The results indicate that low-temperature ($T < 300$ K) thermal conductivity of the moderately doped $(Zn_{1-x}Ag_x)_4Sb_3$ ($x = 0.0025$ and 0.005) reduced remarkably as compared with that of Zn_4Sb_3 due to enhanced impurity (dopant) scattering of phonons. Electrical resistivity and Seebeck coefficient were found to increase first and then decrease obviously with the increase in the Ag content, which could be ascribed to the change of carrier concentration presumably due to different Zn positions occupied by Ag upon increasing doping content. Moreover, the lightly doped compound $(Zn_{0.995}Ag_{0.005})_4Sb_3$ exhibited the best thermoelectric performance due to the improvement in both its electrical resistivity and thermal conductivity, whose figure of merit (at 300 K), ZT, is about 1.3 times larger than that of β-Zn_4Sb_3 obtained in the present study. Present results suggest that proper Ag doping in Zn_4Sb_3 is a promising way of improving its thermoelectric properties.

1. Introduction

Recently, thermoelectric materials have attracted a great deal of attention for their possible application in energy conversion and power generation [1–6]. As one of the prime candidates for thermoelectric application in the moderate temperature range, β-Zn_4Sb_3 has attracted much attention because of its high thermoelectric performance, $ZT = 1.3$ at 670 K [7,8] ($ZT = S^2T/\rho\lambda$, here S, T, ρ and λ are the Seebeck coefficient, the absolute temperature, the electrical resistivity and the total thermal conductivity, respectively), which comes mainly from its extremely low thermal conductivity originating from the structural disorder in its complex crystallographic structure [9,10]. The rhombohedral unit cell of β-Zn_4Sb_3 contains three distinct atomic positions (36 Zn, 18 Sb1, and 12 Sb2 in space group $R\bar{3}c$). Moreover, β-Zn_4Sb_3 manifests disordering in the framework Zn position which displays a considerable occupational deficiency (0.89–0.90), and in the occurrence of three weakly occupied (by around 0.06) general positions representing interstitial Zn atoms [10,11]. The expected ideal composition of the so-called Zn_4Sb_3 is actually $Zn_{13}Sb_{10}$ [11]. However, the composition obtained from the refined occupancies is $Zn_{3.83}Sb_3$ [9] which accords with experimental results [7,8]. In addition, a structural phase transition takes place at about 263 K and β-Zn_4Sb_3 changes reversibly to α-Zn_4Sb_3 below that temperature [12,13]. The study performed by Nylén et al. shows that α-Zn_4Sb_3 is an ordered phase with triclinic unit cell (space group $C\bar{1}$). Moreover, recent researches performed by Nylén et al. [11] have indicated that apart from the β→α phase transition a second low-temperature α→α′ phase transition appears below 235 K, which is deduced to be related to occupational modulation of slightly Zn deficiency in α phase with respect to $Zn_{13}Sb_{10}$ [11].

Nevertheless, although β-Zn_4Sb_3 shows some prospects in thermoelectric applications, there are some imperfections in its properties. Apart from thermal instability at $T > \sim 470$ K [14–16], its figure of merit, ZT, still cannot meet the requirements of practical applications. Hence, further improvements in its properties are imperative. There are many ways of enhancing thermoelectric properties [17]. Among these, doping approach can be used to enhance the thermoelectric properties by reducing its thermal conductivity and adjusting its carrier concentration [18,19]. Recently, doping of Cd, In, Al, Hg, Mg, Nb, Cu, Te and Se [16,20–29] in Zn_4Sb_3 has been reported. These studies showed that when doping with Cd, In or Mg, the thermoelectric performance of Zn_4Sb_3 was not improved obviously. In contrast, the thermoelectric properties were improved substantially after proper doping of Al, Hg, Cu, Nb and Te. Considering the fact that element Ag has fewer valence electrons than Zn, it is expected that an incorporation of Ag in the Zn_4Sb_3 based alloys will largely increase hole concentration and would enhance thermoelectric properties of Zn_4Sb_3. Hence, in the present work, the effects of substitution of Ag for Zn on thermoelectric properties of Zn_4Sb_3 at low temperatures are evaluated and the obtained results are discussed.

2. Experimental procedures

$(Zn_{1-x}Ag_x)_4Sb_3$ ($x = 0$, 0.0025, 0.005, 0.01) compounds were synthesized by the melting and hot-pressing method. The elements (Zn (5N), Sb (3N) and Ag (3N))

* Corresponding author.
E-mail address: xyqin@issp.ac.cn (X.Y. Qin).

0925-8388/$ – see front matter © 2009 Elsevier B.V. All rights reserved.
doi:10.1016/j.jallcom.2009.09.058

were weighed in stoichiometric ratios in a quartz ampule, which was evacuated and sealed. Then the ampules were heated slowly to 1023 K and isothermally kept for 12 h before quenching in water. The obtained compounds were ground in agate mortar to fine powders, which were then compacted by hot-pressing (under a pressure of 600 Mpa) in vacuum at 573 K for 1 h to form bulk samples. The phase structure of the obtained samples was determined by using X-ray diffraction (XRD). Accuracy lattice parameters were measured with XRD by using a Si standard for calibration. Four probes (Cu straps) were electrically and thermally attached to the specimens by silver conductive adhesive paste (Phentex Corp., Ward Hill, MA) to measure their electrical resistance, and when Seebeck coefficient and thermal conductivity were measured the middle two probes were used to explore temperature gradient (difference) and potential difference. All the thermoelectric properties (electrical resistance, Seebeck coefficient and thermal conductivity) were measured simultaneously by using a physical property measurement system (PPMS, Quantum Design) in the temperature range from 15 to 300 K. The densities of the hot-pressed samples were measured in alcohol by using Archimedes method. The relative densities of $(Zn_{1-x}Ag_x)_4Sb_3$ ($x = 0$, 0.0025, 0.005, 0.01) were 97.3%, 97.1%, 97.4% and 98.1% of the theoretical density (6.36 g cm^{-3}), respectively.

3. Results and discussion

3.1. Sample characterization

X-ray diffraction patterns at room-temperature for all the samples are shown in Fig. 1. It can be seen that for $(Zn_{1-x}Ag_x)_4Sb_3$ samples (with $x = 0$, 0.0025, 0.005), the main diffraction peaks correspond to β-Zn_4Sb_3 (JCPD No.34-1013) phase, no other phase being detected obviously from the XRD patterns. Whereas, a small amount of ZnSb phase was detected for the $(Zn_{1-x}Ag_x)_4Sb_3$ with $x = 0.01$, as indicted in the figure. Accurate lattice parameter measurement indicates that lattice constants a and c increases monotonically with increasing Ag content (Fig. 2a). Moreover, as the Ag content x increase from 0 to 0.01, the ratio c/a decreases from 1.01695 to 1.01626 (Fig. 2b), being consistent with the experimental data for Cd doping in Zn_4Sb_3 obtained by Nakamoto et al. [21]. Present result indicates that substitution of Ag for Zn occurs, leading to the formation of $(Zn_{1-x}Ag_x)_4Sb_3$ compounds.

3.2. The resistivity and Seebeck coefficient

The electrical resistivity versus temperature for $(Zn_{1-x}Ag_x)_4Sb_3$ ($x = 0$, 0.0025, 0.005, 0.01) in the range of 14–300 K is presented in Fig. 3a. The room-temperature resistivity (3.4 mΩ cm) of β-Zn_4Sb_3 obtained here is 4 times larger than that (0.8 mΩ cm) reported by Souma et al. [30] for their β-Zn_4Sb_3. Such a difference may arise because of the difference in microstructures (such as porosity and grain sizes) of the samples obtained by using different sintering techniques (hot-pressing was used in the present study, whereas spark plasma sintering was used by Souma et al. [30]). One can see that the temperature dependence of the resistivity for the four samples is similar: The resistivitiy shows basically metallic-like (i.e., $d\rho/dT > 0$) behavior in the whole temperature range measured, indicating that they all belong to a degenerated semiconductor. The observed anomaly in the ρ–T curve for Zn_4Sb_3 between 263 and 233 K is associated with the structural transition from β to α/α′ phase [21,30].

As compared with Zn_4Sb_3, the resistivity of the lightly doped sample with $x = 0.0025$ increases remarkably. However, with increasing Ag content x from 0.0025 to 0.01, the resistivity of $(Zn_{1-x}Ag_x)_4Sb_3$ decreases monotonically. For instance, the room-temperature resistivity decreases from 5.9 mΩ cm for $x = 0.0025$ to 3.2 mΩ cm for $x = 0.005$ and to 2.9 mΩ cm for $x = 0.005$. This increase or decrease in the resistivity after doping with different amount of Ag contents would come from changes of carrier concentration caused by substitution of Ag for Zn [31]. Fig. 3b shows the magnified plots of ρ–T for the four samples in the temperature range from 235 to 290 K. It shows that the increase of ρ associated

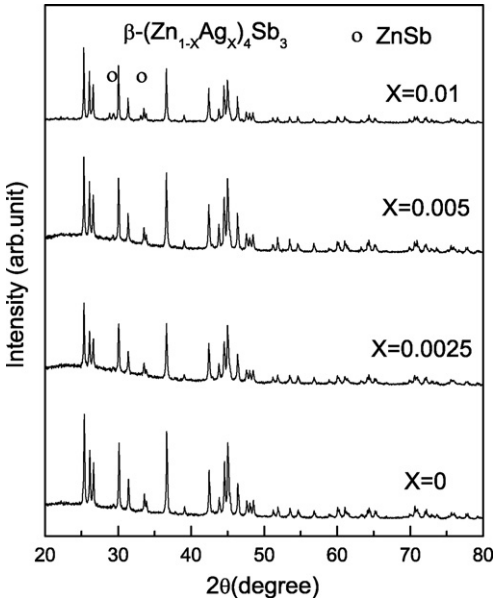

Fig. 1. XRD patterns (Cu Kα irradiation) of $(Zn_{1-x}Ag_x)_4Sb_3$ ($x = 0$, 0.0025, 0.005, 0.01) at R.T.

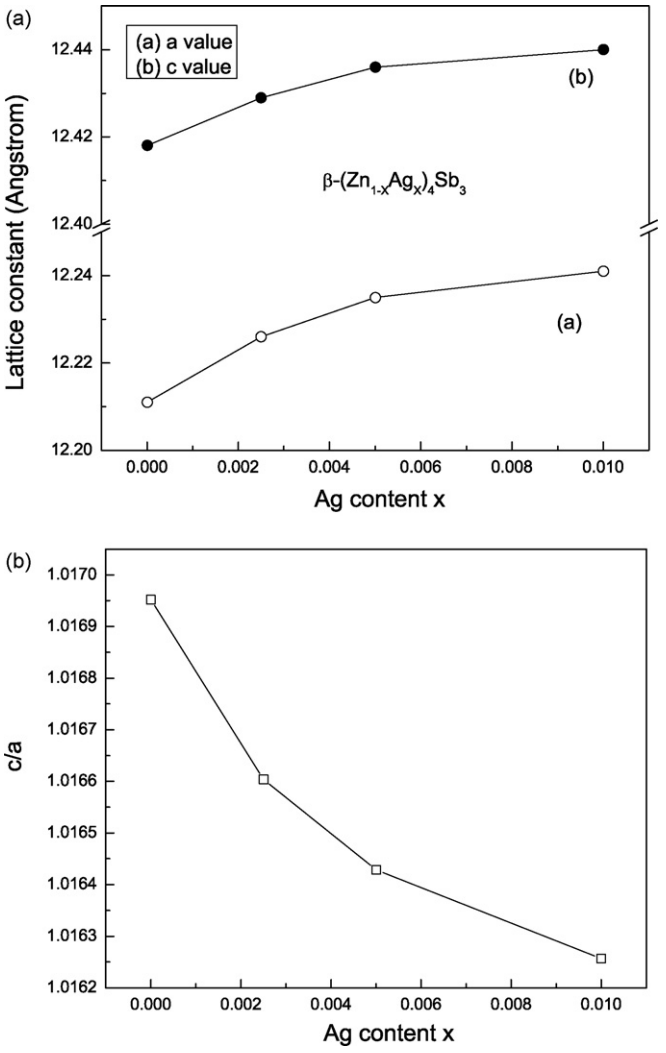

Fig. 2. (a) Composition (x) dependence of lattice parameters a and c for $(Zn_{1-x}Ag_x)_4Sb_3$ ($x = 0$, 0.0025, 0.005, 0.01) at R.T. (b) Lattice parameters c/a value of $(Zn_{1-x}Ag_x)_4Sb_3$ as a function of Ag content x at R.T.

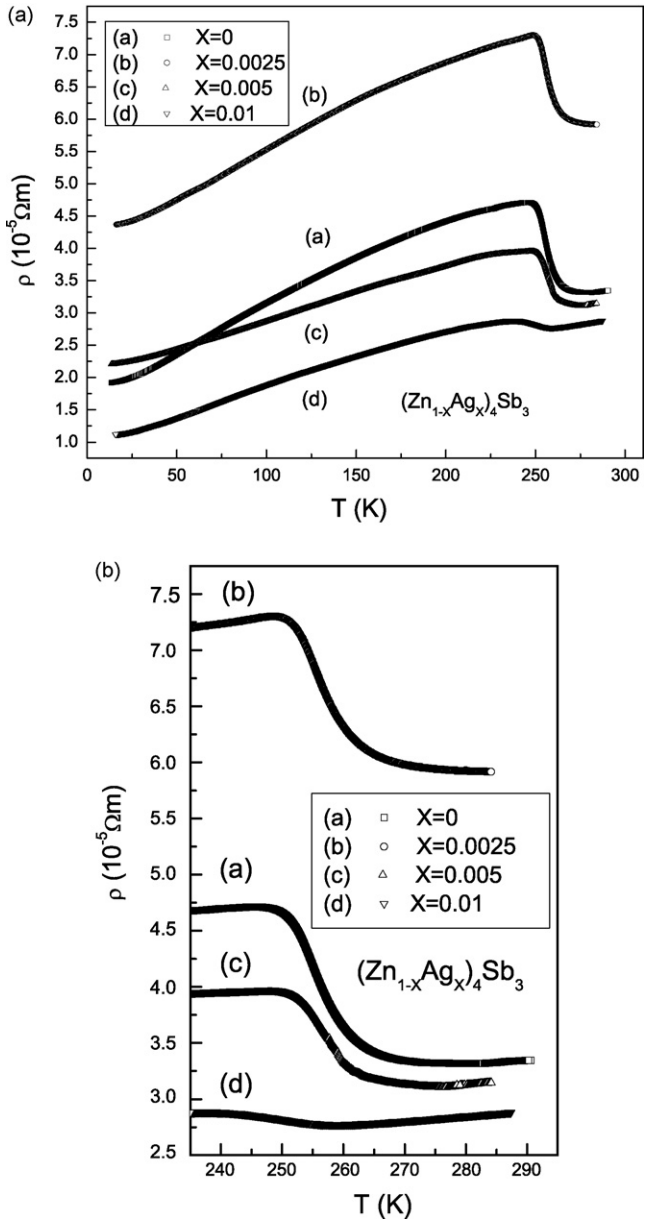

Fig. 3. (a) The temperature dependence of the electrical resistivity ρ for $(Zn_{1-x}Ag_x)_4Sb_3$: (a) $x = 0$, (b) $x = 0.0025$, (c) $x = 0.005$, (d) $x = 0.01$. (b) The magnified plots of the resistivity of four samples from 235 to 290 K.

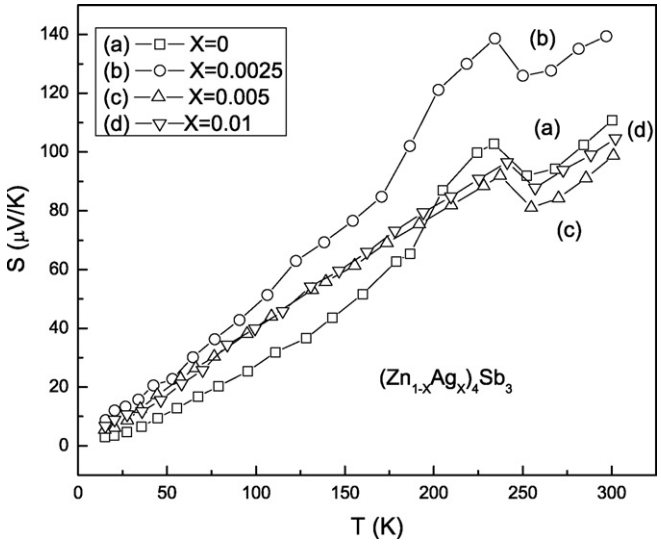

Fig. 4. Variation of Seebeck coefficients S with temperature for $(Zn_{1-x}Ag_x)_4Sb_3$: (a) $x = 0$, (b) $x = 0.0025$, (c) $x = 0.005$, (d) $x = 0.01$.

with the β to α phase transition decreases with increasing Ag content ($\Delta\rho = 1.39$, 1.38, 0.84 and 0.11 mΩ cm for $x = 0$, 0.0025, 0.005 and 0.01, respectively), implying that the change of carrier concentration or/and scattering rate accompanying β→α phase transition diminishes with increasing Ag content [31].

The temperature dependences of Seebeck coefficient for $(Zn_{1-x}Ag_x)_4Sb_3$ are shown in Fig. 4. The positive values of the Seebeck coefficient of the samples mean that the major charge carriers in all the samples are holes. The Seebeck coefficient (110.8 μV/K) of β-Zn_4Sb_3 at room-temperature obtained here is smaller than that reported by Souma et al. [30] for their β-Zn_4Sb_3. Such a difference may also arise due to the difference in microstructures of the samples obtained by using different sintering techniques [30]. It can be seen clearly that the temperature dependence of Seebeck coefficient of all the samples is similar: it decreases with decreasing temperature, but increases abruptly at 250 K and then continues to decrease with further decreasing temperature, leaving a maximum at ~230 K, which can reasonably be ascribed to the β→α/α′ phase transition [30]. In addition, one finds that Seebeck coefficient of $(Zn_{1-x}Ag_x)_4Sb_3$ ($x = 0.0025$) is obviously larger than that of Zn_4Sb_3, but it decreases with further increase of Ag content. For instance, room-temperature Seebeck coefficient decreases from 139.5 μV/K for $x = 0.0025$ to 98.8 μV/K for $x = 0.005$. However, the Seebeck coefficient of $(Zn_{1-x}Ag_x)_4Sb_3$ increases from 98.8 μV/K for $x = 0.005$ to 104.6 μV/K for $x = 0.01$.

The non-monotonic change behavior of the resistivity and thermopower with increasing Ag content could originate from local structure, i.e., specific locations occupied by Ag atoms. As mentioned above, besides normal lattice Zn the unit cell of β-Zn_4Sb_3 contains interstitial Zn and normal Zn lattice vacancies [9,10]. Therefore, dopants can be incorporated in many ways in β-Zn_4Sb_3. That is, upon doping Ag may replace three different kinds of species, i.e., Zn atoms in normal lattice, interstitial Zn atoms and normal lattice (Zn) vacancies. Since dopant Ag has the electronic structure $[Kr]4d^{10}5s^1$, if it replaces a normal lattice Zn or interstitial Zn ($[Ar]3d^{10}4s^2$) atom, an acceptor level in the band gap will be introduced, resulting in an increase in the hole concentration. This would have happened in the case of heavily doped compounds $(Zn_{1-x}Ag_x)_4Sb_3$ (with $x = 0.005$–0.01), for the resistivity and Seebeck coefficient of $(Zn_{1-x}Ag_x)_4Sb_3$ ($x = 0.005$–0.01) decreases as compared to those of the un-doped compound. However, present explanation is inconsistent with phenomenon observed in the lightly doped compound $(Zn_{0.9975}Ag_{0.0025})_4Sb_3$, whose Seebeck coefficient and the resistivity are substantially larger than those of un-doped Zn_4Sb_3 (curve (b) in Figs. 3 and 4). This suggests that in the case of lightly doping Ag atoms could mainly fill in the Zn vacancies in the normal sites. In fact, previous studies [7,9] showed that β-Zn_4Sb_3 is always zinc deficient with the formula $Zn_{3.9-\delta}Sb_3$ ($0 < \delta < 0.02$), which means that there are not only lattice Zn vacancies accompanied by interstitial Zn [11,32] but also independent Zn vacancies (which are not (or fully) accompanied by interstitial Zn atoms nearby). These independent Zn vacancies are expected to be filled preferentially by Ag atoms in consideration of energy changes. Obviously, as Ag fill the Zn vacancies the corresponding acceptor levels will be eliminated or reduced, resulting in decrease in hole concentration of the doped compound (and giving rise to increase of the resistivity and Seebeck coefficient). Since the number of the independent normal Zn vacancies is very limited, as dopant content increases substitution of Ag for Zn atoms in normal lattice

and/or interstitial sites will become dominant, which would lead to increase in hole concentration, as manifested in the decrease of the resistivity and Seebeck coefficient (as observed in the heavily doped compounds (Fig. 3)).

It is worthwhile to point out that there are possibilities that the non-monotonic behavior of the resistivity and thermopower with increasing Ag would be related to other factors. Recently, Litvinchuk et al. and Nylén et al. [31,33] studied structural transition behavior and transport properties of Bi, Sn and Pb doped Zn_4Sb_3 compounds, and they showed that metal doping caused an obvious change in the ratio of Zn/Sb, which led to not only changes of their structural transition behavior, but also changes of carrier concentration and scattering rate [31,33]. If Ag doping causes increase (or decrease) in interstitial Zn atoms (or Zn/Sb ratio) in the material preparation, the carrier (hole) concentration in Zn_4Sb_3 will decrease (or increase). However, since in our sample preparation the mass of Zn and Sb are fixed according to stoichiometric ratios, the fluctuation in the ratio of Zn/Sb would not be remarkable. Even if the change of Zn/Sb ratio happens, it is difficult for one to imagine a non-monotonic change of the ratio with increasing Ag content. Nevertheless, a small quantity of ZnSb impurity phase is detected in the heavily doped sample $(Zn_{0.99}Ag_{0.01})_4Sb_3$ (Fig. 1). This means that Zn/Sb ratio in this sample will increase due to precipitation of ZnSb phase, leading to increase in the number of interstitial Zn atoms and decrease of hole concentration. This speculation is, instead, inconsistent with the observed phenomenon in which the resistivity and Seebeck coefficient decrease substantially as compared to those of lightly doped samples (Figs. 3 and 4). Therefore, the possible change of Zn/Sb ratio accompanied with Ag doping (if any) could hardly account for the non-monotonic behavior of the resistivity and thermopower. Likewise, one has difficulties to explain this non-monotonic behavior in terms of change of the scattering rate at different doping levels, for scattering rate usually increases with increasing dopant content due to enhanced potential disorder, leading to decrease in its carrier mobility (and consequently increase in its electrical resistivity).

3.3. The thermal conductivity and the dimensionless figure of merit

The temperature dependences of total thermal conductivity λ for $(Zn_{1-x}Ag_x)_4Sb_3$ ($x = 0$, 0.0025, 0.005, 0.01) are shown in Fig. 5. It can be seen that the temperature behavior of the thermal conductivity for all the samples is similar: it increases with increasing temperature and then decreases with further increasing temperature up to ~230 K, leaving a maximum locating at a certain temperature (at 35, 33, 57 and 27 K for $(Zn_{1-x}Ag_x)_4Sb_3$ ($x = 0$, 0.0025, 0.005, 0.01), respectively). In contrast, however, the thermal conductivity of the substituted compounds decreases remarkably as compared with Zn_4Sb_3. The total thermal conductivity of a solid is the sum of a lattice thermal conductivity (λ_L) and a carrier thermal conductivity (λ_C): $\lambda = \lambda_L + \lambda_C$. λ_C can be estimated using the Wiedemann-Franz law, i.e., $\lambda_C = L_0 T/\rho$ (here L_0 and ρ are the Lorenz number and the electrical resistivity, respectively). Hence, the lattice thermal conductivity of $(Zn_{1-x}Ag_x)_4Sb_3$ can be obtained from λ_L and λ_C, as given in Fig. 6. The inset of Fig. 6 presents the carrier thermal conductivity as a function of temperature for $(Zn_{1-x}Ag_x)_4Sb_3$. It can be seen from the inset of Fig. 6 that λ_C increases slowly with increasing temperature at $T < 250$ K and then it rises rapidly with a further increase in temperature. However, λ_C is much smaller than λ_L over the whole temperature range. This result indicates that the thermal conductivity of $(Zn_{1-x}Ag_x)_4Sb_3$ is mainly determined by its lattice contribution. The value of the lattice thermal conductivity corresponding to the low-temperature peak for Zn_4Sb_3, $(Zn_{0.9975}Ag_{0.0025})_4Sb_3$, $(Zn_{0.995}Ag_{0.005})_4Sb_3$, $(Zn_{0.99}Ag_{0.01})_4Sb_3$ is 2.58, 1.67, 1.18 and 3.16 $W m^{-1} K^{-1}$, respectively. Obviously, low-temperature lattice thermal conductivity of the doped compounds reduces remarkably as compared with that of Zn_4Sb_3, and the more the doped Ag content, the lower the lattice conductivity (curves a, b and c). The obviously lower lattice thermal conductivity of the compound $(Zn_{1-x}Ag_x)_4Sb_3$ ($x = 0.0025$ and 0.005) as compared with Zn_4Sb_3 can be ascribed to the enhancement of phonon scattering by impurity (Ag) atoms with greater atomic weight. However, one notices that the low-temperature lattice thermal conductivity of $(Zn_{0.99}Ag_{0.01})_4Sb_3$ is even larger than Zn_4Sb_3. This large lattice thermal conductivity observed for $(Zn_{0.99}Ag_{0.01})_4Sb_3$ can be attributed to the contribution of impurity phase ZnSb (Fig. 1), for ZnSb phase has a much higher lattice thermal conductivity (2.26 $W m^{-1} K^{-1}$) [34] than that of Zn_4Sb_3. In fact, the contribution of impurity phase ZnSb can also be detected from Seebeck coefficient measurements. By comparing curve c with curve d in Fig. 4, one notices that Seebeck coefficient of $(Zn_{0.99}Ag_{0.01})_4Sb_3$ is slightly larger than that of $(Zn_{0.995}Ag_{0.005})_4Sb_3$. This increase in Seebeck coefficient

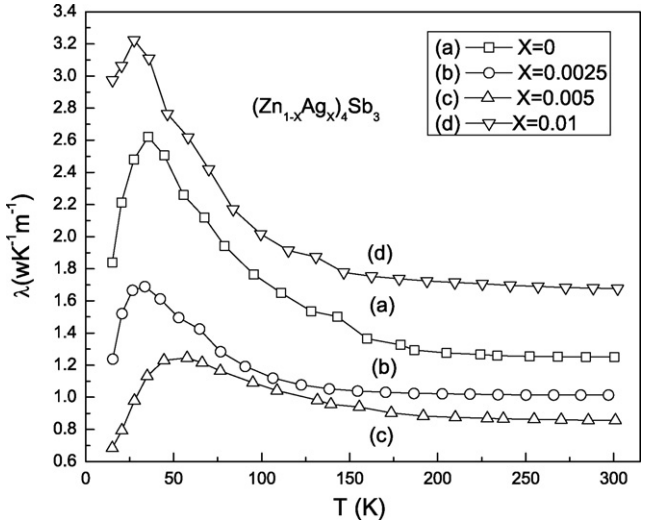

Fig. 5. Variation of thermal conductivity λ with temperature for $(Zn_{1-x}Ag_x)_4Sb_3$: (a) $x = 0$, (b) $x = 0.0025$, (c) $x = 0.005$, (d) $x = 0.01$.

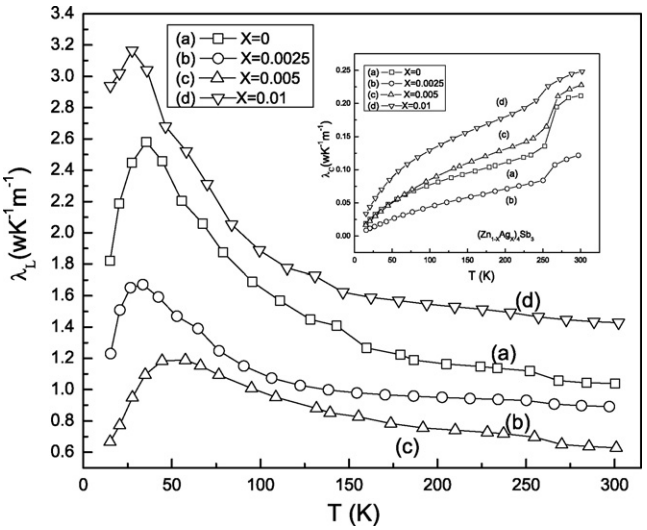

Fig. 6. Variation of lattice thermal conductivity λ_L with temperature for $(Zn_{1-x}Ag_x)_4Sb_3$: (a) $x = 0$, (b) $x = 0.0025$, (c) $x = 0.005$, (d) $x = 0.01$. The inset shows the carrier thermal conductivity λ_C as a function of temperature for $(Zn_{1-x}Ag_x)_4Sb_3$: (a) $x = 0$, (b) $x = 0.0025$, (c) $x = 0.005$, (d) $x = 0.01$.

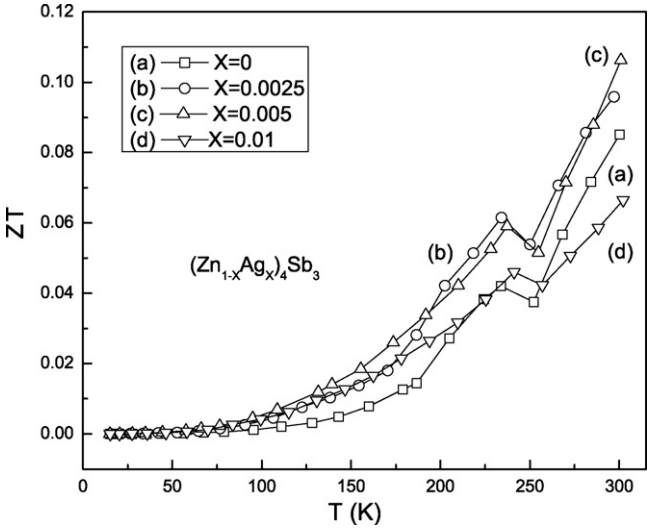

Fig. 7. The temperature dependence of ZT for $(Zn_{1-x}Ag_x)_4Sb_3$: (a) $x = 0$, (b) $x = 0.0025$, (c) $x = 0.005$, (d) $x = 0.01$.

could reasonably be ascribed to the contribution of the higher Seebeck coefficient of the ZnSb phase (196 μV/K) [34] contained in $(Zn_{0.99}Ag_{0.01})_4Sb_3$ sample.

The thermoelectric properties are summed up by the dimensionless figure of merit ZT, which is shown in Fig. 7. The temperature behavior of ZT for all samples shows a valley at the temperature around 253 K due to $\beta \leftrightarrow \alpha/\alpha'$ phase transition. The ZT for the heavy substituted compound $(Zn_{0.99}Ag_{0.01})_4Sb_3$ is smaller than that of pure β-Zn_4Sb_3 at temperatures above 250 K. This is mainly due to its considerably larger thermal conductivity and smaller Seebeck coefficient, although its electrical resistivity is improved as compared to that of the un-doped compound. On the other hand, the ZT of the lightly substituted compounds $(Zn_{0.9975}Ag_{0.0025})_4Sb_3$ and $(Zn_{0.995}Ag_{0.005})_4Sb_3$ shows significant improvement in the whole temperature range investigated. In particular, the ZT value of $(Zn_{0.995}Ag_{0.005})_4Sb_3$ reaches a value of 0.106, which is about 1.3 times larger than that of pure Zn_4Sb_3 at 300 K. Obviously, this improvement in the thermoelectric properties of $(Zn_{0.995}Ag_{0.005})_4Sb_3$ originates from the decrease in both the electrical resistivity and lattice thermal conductivity, which can be ascribed to the increased holes concentration and enhanced phonon scattering due to substitution of Ag for Zn.

4. Conclusions

The thermoelectric properties of Ag-doped compounds $(Zn_{1-x}Ag_x)_4Sb_3$ have been studied. The results indicate that low-temperature ($T < 300$ K) thermal conductivity λ of the lightly doped $(Zn_{1-x}Ag_x)_4Sb_3$ ($x = 0.0025$ and 0.005) reduces remarkably as compared with that of Zn_4Sb_3 presumably due to enhanced impurity (dopant) scattering of phonons. The larger low-temperature lattice thermal conductivity of $(Zn_{0.99}Ag_{0.01})_4Sb_3$ as compared with that of Zn_4Sb_3 could be attributed to the contribution of impurity phase ZnSb. The resistivity ρ and Seebeck coefficient S are found to increase and then decrease moderately with the increase in the Ag content, which could be ascribed to change of carrier concentration due to different positions occupied by Ag upon increasing doping content. Moreover, the lightly doped compound $(Zn_{0.995}Ag_{0.005})_4Sb_3$ exhibits the best thermoelectric performance due to the improvement in both its electrical resistivity and thermal conductivity, whose ZT (at 300 K) is about 1.3 times larger than that of β-Zn_4Sb_3 obtained in the present study. Present results suggest that proper Ag doping in Zn_4Sb_3 is a promising way of improving its thermoelectric properties.

Acknowledgement

Financial support from National Natural Science Foundation of China (No. 10774145, No. 50472097 and No. 10504034) is gratefully acknowledged.

References

[1] M. Takashiri, S. Tanaka, M. Takiishi, M. Kihara, K. Miyazaki, H. Tsukamoto, J. Alloys Compd. 462 (2008) 351–355.
[2] J.L. Mi, X.B. Zhao, T.J. Zhu, J. Ma, J. Alloys Compd. 452 (2008) 225–229.
[3] K. Ozga, K. Nouneh, A. Slezak, I.V. Kityk, J. Alloys Compd. 448 (2008) 49–52.
[4] K. Park, J.K. Seong, S. Nahm, J. Alloys Compd. 455 (2008) 331–335.
[5] P.H. Xiang, Y. Kinemuchi, H. Kaga, K. Watari, J. Alloys Compd. 454 (2008) 364–369.
[6] M.A. Mcguire, A.S. Malik, F.J. Disalvo, J. Alloys Compd. 460 (2008) 8–12.
[7] T. Caillat, J.P. Fleurial, A. Borshevsky, J. Phys. Chem. Solids 58 (1997) 1119–1125.
[8] M. Chitroub, F. Besse, H. Scherrer, J. Alloys Compd. 460 (2008) 90–93.
[9] G.J. Snyder, M. Christensen, E. Nishibori, T. Caillat, B.B. Iversen, Nat. Mater. 3 (2004) 458–463.
[10] J. Nylén, M. Andersson, S. Lidin, U. Häussermann, J. Am. Chem. Soc. 126 (2004) 16306–16307.
[11] J. Nylén, S. Lidin, M. Andersson, B.B. Iversen, H. Liu, N. Newman, U. Häussermann, Chem. Mater. 19 (2007) 834–838.
[12] H.W. Mayer, I. Mikhail, K. Schubert, J. Less Common Met. 59 (1978) 43–52.
[13] M. Tapiero, S. Tarabichi, J.G. Gies, C. Noguet, J.P. Zielinger, M. Joucla, J. Loison, M. Robino, Sol. Energy Mater. 12 (1985) 257–274.
[14] Y. Mozharivskyj, Y. Janssen, J.L. Harringa, A. Kracher, A.O. Tsokol, G.J. Miller, Chem. Mater. 18 (2006) 822–831.
[15] B.L. Pedersen, B.B. Iversen, Appl. Phys. Lett. 92 (2008) 161907.
[16] B.L. Pedersen, H. Birkedal, M. Nygren, P.T. Frederiksen, B.B. Iversen, J. Appl. Phys. 105 (2009) 013517.
[17] M.S. Dresslhaus, G. Chen, M.Y. Tang, R. Yang, H. Lee, D.Z. Wang, Z.F. Ren, J.P. Fleurial, P. Gogna, Adv. Mater. 19 (2007) 1043–1053.
[18] G.D. Mahan, J. Appl. Phys. 65 (1989) 1578–1583.
[19] T. Ueda, K. Hasezaki, J. Electron. Mater. 38 (2009) 1025–1029.
[20] F. Liu, X.Y. Qin, H.X. Xin, J. Phys. D: Appl. Phys. 40 (2007) 7811–7816.
[21] G. Nakamoto, T. Souma, M. Yamaba, M. Kurisu, J. Alloys Compd. 377 (2004) 59–65.
[22] V.L. Kuznetsov, D.M. Rowe, J. Alloys Compd. 372 (2004) 103–106.
[23] B.L. Pedersen, H. Birkedal, E. Nishibori, A. Bentien, M. Sakata, M. Nygren, P.T. Frederiksen, B.B. Iversen, Chem. Mater. 19 (2007) 6304–6311.
[24] D. Li, H.H. Hng, J. Ma, X.Y. Qin, J. Mater. Res. 24 (2009) 430–435.
[25] J.L. Cui, H. Fu, L.D. Mao, D.Y. Chen, X.L. Liu, J. Appl. Phys. 106 (2009) 023702.
[26] W. Li, L.M. Zhou, Y.L. Li, J. Jiang, G.J. Xu, J. Alloys Compd. (2008), doi:10.1016/j.jallcom.2009.06.145.
[27] H.J. Gau, J.L. Yu, C.C. Wu, Y.K. Kuo, C.H. Ho, J. Alloys Compd. 480 (2009) 73–75.
[28] T. Ueda, C. Okamura, K. Hasezaki, J. Jpn. Inst. Met. 73 (2009) 487–490.
[29] J.L. Cui, H. Fu, D.Y. Chen, L.D. Mao, X.L. Liu, W. Yang, Mater. Charact. 60 (2009) 824–828.
[30] T. Souma, G. Nakamoto, M. Kurisu, J. Alloys Compd. 340 (2002) 275–280.
[31] A.P. Litvinchuk, J. Nylén, B. Lorenz, A.M. Guloy, U. Häussermann, J. Appl. Phys. 103 (2008) 123524.
[32] F. Cargnoni, E. Nishibori, P. Rabiller, L. Bertini, G.J. Snyder, M. Christensen, C. Gatti, B.B. Iversen, J. Chem. Eur. 10 (2004) 3861–3870.
[33] J. Nylén, S. Lidin, M. Andersson, H.X. Liu, N. Newman, U. Häussermann, J. Solid State Chem. 180 (2007) 2603–2615.
[34] L.T. Zhang, M. Tsutsui, K. Ito, M. Yamaguchi, J. Alloys Compd. 358 (2003) 252–256.